DOI: https://doi.org/10.5592/CO/EUROENGEO.2024.182

SURFACE DEFORMATION OF THE LANDSLIDE OF HATTARO PASS CAUSED BY THE 2024 NOTO PENINSULA EARTHQUAKE

TERUYUKI KIKUCHI [1], KEIJI CHIDA [2], JUN TAJIKA [3], KENTARO KANAYAMA [4], KOSUKE OTSU [5], TERUYOSHI HATANO [6], SHIN ANDO [7], NOBUSUKE HASEGAWA [7], HIDEKI INAGAKI [8], MASAHIKO OSADA [9]

[1] *Suwa University of Science, Japan, kikuchi_teruyuki@rs.sus.ac.jp*

[2] *Hassu Co., Ltd., Japan, k-chida@hasshu.co.jp*

[3] *Geo-technical Research Co. Ltd., Japan, tajika@geo-tech.co.jp*

[4] *Dia Nippon Engineering Consultants Co., Ltd., Japan, kanayama_kentaro@dcne.co.jp*

[5] *Docon Co., Ltd., Japan, ko1974@docon.jp*

[6] *Nakanihon Air Co. Ltd., Japan, teruyoshi.hatano@nnk.co.jp*

[7] *Oyo Co. Ltd, Japan, ando-shin@oyonet.oyo.co.jp, hasegawa-nobu@oyonet.oyo.co.jp*

[8] *Kankyo Chishitsu Co., Ltd., Japan, inagaki@kankyo-c.com*

[9] *Saitama University, Japan, osada@mail.saitama-u.ac.jp*

Abstract

This study aimed to confirm that the occurrence of specific surface deformations is consistent with actual geological structures. Although it is difficult to obtain an overall understanding of large-scale land surface deformations, particularly from field surveys alone, the interpretation of land surface deformations through vector analysis can lead to a correct understanding. This makes the role of estimations based on topography, geology, and history more important for predicting and forecasting landslides and slope failures. In this study, we focused on a landslide that occurred west of the *Hattaro* Pass on the boundary between *Wajima* and *Suzu* cities during the 2024 *Noto* Peninsula Earthquake (Mj7.6) on January 1, 2024. The results of the multitemporal vector analysis and the views obtained from the field survey are summarized.

Key words

Noto Peninsula Earthquake, Landslide, Displacement vector analysis, Syncline

1 Introduction

In recent years, disasters associated with extreme weather events and large-scale earthquakes have occurred frequently and are expected to continue in the future. In such large-scale disasters, slope disasters of various sizes and forms, such as deep and surface failures, have been reported (Yin et al., 2009; Wartman et al., 2013; Karakas et al., 2021).

After a disaster, it is effective to quickly identify land surface changes and prevent the occurrence of secondary disasters for the stability of social infrastructure. Furthermore, it is difficult to understand the mechanism of disaster occurrence when the target area and number of sites are large (Osanai et al., 2019). In particular, when many landslides and collapses occur simultaneously, they are impossible to monitor using ordinary extensometers and inclinometers in terms of securing materials and costs, and multiple locations over a wide area must be monitored in detail. Aerial laser surveying, a quality-controlled method, can be used to measure land surface changes during a disaster by processing data from two different periods. For example, sediment change maps and volume calculations can be created by calculating the elevation range of the same coordinates from two periods of digital elevation model

(DEM) data. Vector analysis has been used to study landslides and mass movements associated with earthquakes and heavy rainfall disasters (Mukoyama, 2010; Kikuchi et al., 2017). Using the same precision laser measurement results obtained before and after a disaster, this method can examine the process of change in a target area and obtain results that can lead to the prediction of future changes. Vector analysis is useful for understanding geological structures and landslide mechanisms.

Landslide sliding has been linked to geological structures. The Monte Tok landslide movement that caused the 1963 Vaiont Dam failure highlights the importance of structural folding (Massironi et al., 2013). Landslide behavior is also related to sensitivity to crustal deformation, and structural conditions can indirectly influence landslides (Damm et al., 2010).

The aim of this study was to confirm whether the specific landslide locations obtained from the analysis of the variation vectors of bi-period aerial laser surveys were consistent with the actual geological phenomena in the area. Although it is difficult to understand the entirety of a land surface change, particularly at a large-scale, using field surveys alone, the interpretation of the land surface change can lead to a correct understanding by performing a variation vector analysis (Takami et al., 2019). Increasing the number of case studies makes the role of estimations based on topography, geology, and past history more important in the prediction of landslides, slope failures, and their occurrence.

In this study, we examined a landslide that occurred west of the *Hattaro* Pass on the boundary between *Wajima* City and *Suzu* City during the 2024 *Noto* Peninsula Earthquake (Mj7.6) on January 1, 2024 (Figure 1). The results of the multitemporal vector analysis and the views obtained from the field survey are summarized.

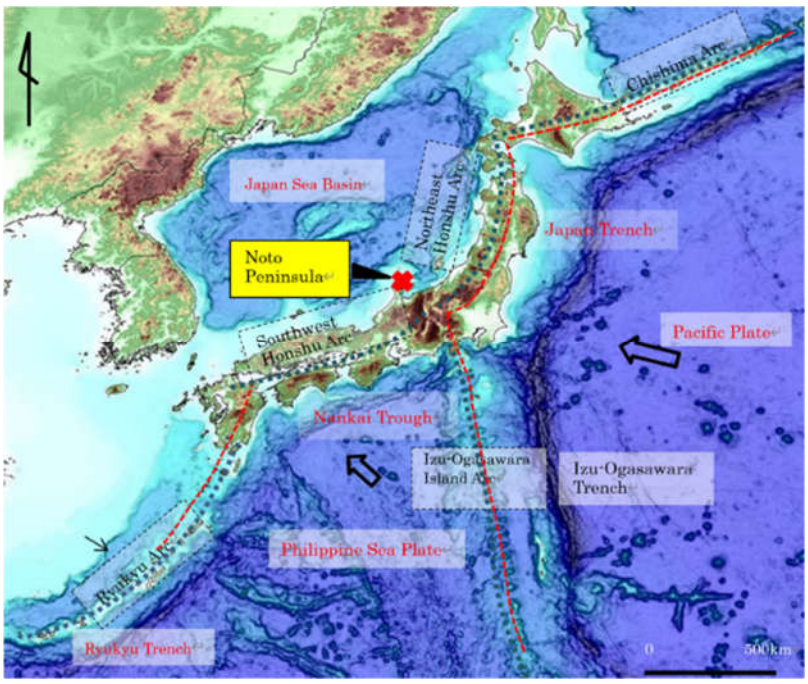

Figure 1. General topographic view around Japan

2 Disaster Event

The 2024 *Noto* Peninsula Earthquake occurred on January 1st, 2024, with a maximum intensity of VII in northwestern Japan. The earthquake had a magnitude of 7.6 at a depth of approximately 15 km in the *Noto* region of *Ishikawa* Prefecture. The seismic mechanism of this earthquake was a reverse fault type with maximum principal stress axis in northwest-southeast direction, and the earthquake occurred within the crust. Figure 1 presents a general view of Japan. The Japanese Archipelago comprises five island arcs. The Philippine Sea Plate moves in the NW direction at 4 cm/yr and subducts into the *Nankai*

Trough. Conversely, the Pacific Plate moves in the WNW direction at 9 cm/yr on average and subducts in the Japan and *Izu-Ogasawara* trenches. Moreover, the *Izu-Ogasawara* Island Arc collided with the Honshu Arc and intruded to the north. These continuous movements in the subduction zones at the boundaries of the plates are the main causes of large earthquakes and tsunamis. Many active faults are distributed in the island arcs.

3 Topography and Geology

The target site is located west of *Hattaro* Pass, approximately 4 km northwest of *Horyu-san* (471 m), at the boundary between *Wajima* City and *Suzu* City, *Ishikawa* Prefecture, in the northeastern *Noto* Peninsula, as shown in Figure 2. This mountain range has a summit approximately 400 m above sea level and many gentle slopes. The area is composed of siliceous Neogene mudstones. The oblique axis of the *Wakayama-gawa* syncline gently west-southwest from the *Wakayama* River to the *Suzuya* River via the *Hattaro* Pass (Yoshikawa et al., 2002). This area was the site of many landslides caused by the 2024 *Noto* Peninsula Earthquake (Geospatial Information Authority of Japan, 2024).

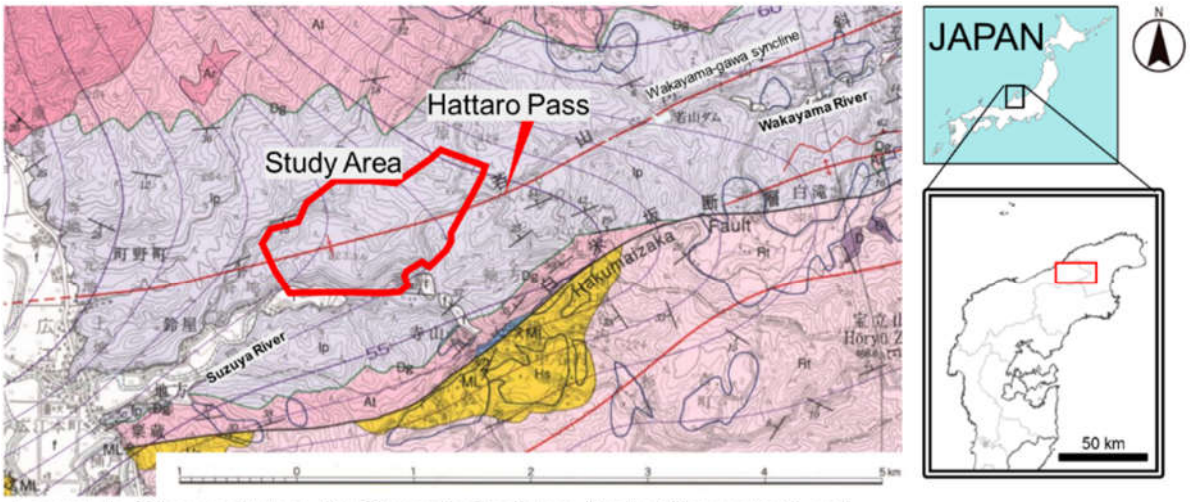

Figure 2. Geological map and survey location map: Geology of the *Suzumisaki, Noto-iida* and *Horyuzan* district., in: Quadrangle Series, 1:50,000 (Yoshikawa et al., 2002)

4 Displacement Vector Analysis Method and Results

In this study, displacement vector analysis was conducted using the pre- and post-earthquake point-cloud data shown in Table 1. Compared to the usual difference analysis for height, the variation vector analysis method provides a concrete understanding of the direction of variation and has been increasingly used in recent years (Fey et al., 2015). The displacement vector analysis method is based on a point cloud-matching process in which the point clouds of the lower model (Substratum-DEM) are compared directly without meshing (Kikuchi et al., 2017). Pre-earthquake data for 2020/2022 were used as the first period, and post-earthquake data were used as the second period. The point with the highest agreement was used as the final displacement (Figure 3). For locations where the displacement is greater than 10 m, that is where the land surface has changed to the extent that matching is not possible, the displacement vector cannot be calculated. Therefore, the results of the height difference analysis, shown in Figure 4, were used to confirm the results.

The size of the landslide variation area reached approximately 1.6 km east-west and 1.1 km north-south

in the analysis area, which is comparable in scale to the *Aratosawa* seismic landslide of the *Miyagi-Iwate Nairiku* Earthquake (2008, Mj7.2) (Kinoshita et al., 2012), although the magnitude of the variation differs. The displacement of the moving body exceeded 5 m in many locations, and the direction of displacement was in the southern direction; however, westward and eastward displacements were also observed at several locations, reflecting the complex ground deformation during the earthquake. Based on the results of displacement vector analysis, the moving body, including the collapse site, can be divided into multiple blocks. The results of the displacement vector analysis were classified using the same trend vectors. As a result, they can be summarized into nine blocks, as shown in Figure 5. These blocks are predominantly moved from south to south-southwest, though several are moved west to southwest.

Table 1. List of data used for aerial laser surveys

Type of data	pre-earthquake	post-earthquake
Time of survey	2020, 2022	1/11/2024
Average point density	18 point/m^2	18 point/m^2
Provider	APIGD*	Nakanihon Air Co. Ltd.

* Association for Promotion of Infrastructure Geospatial information Distribution

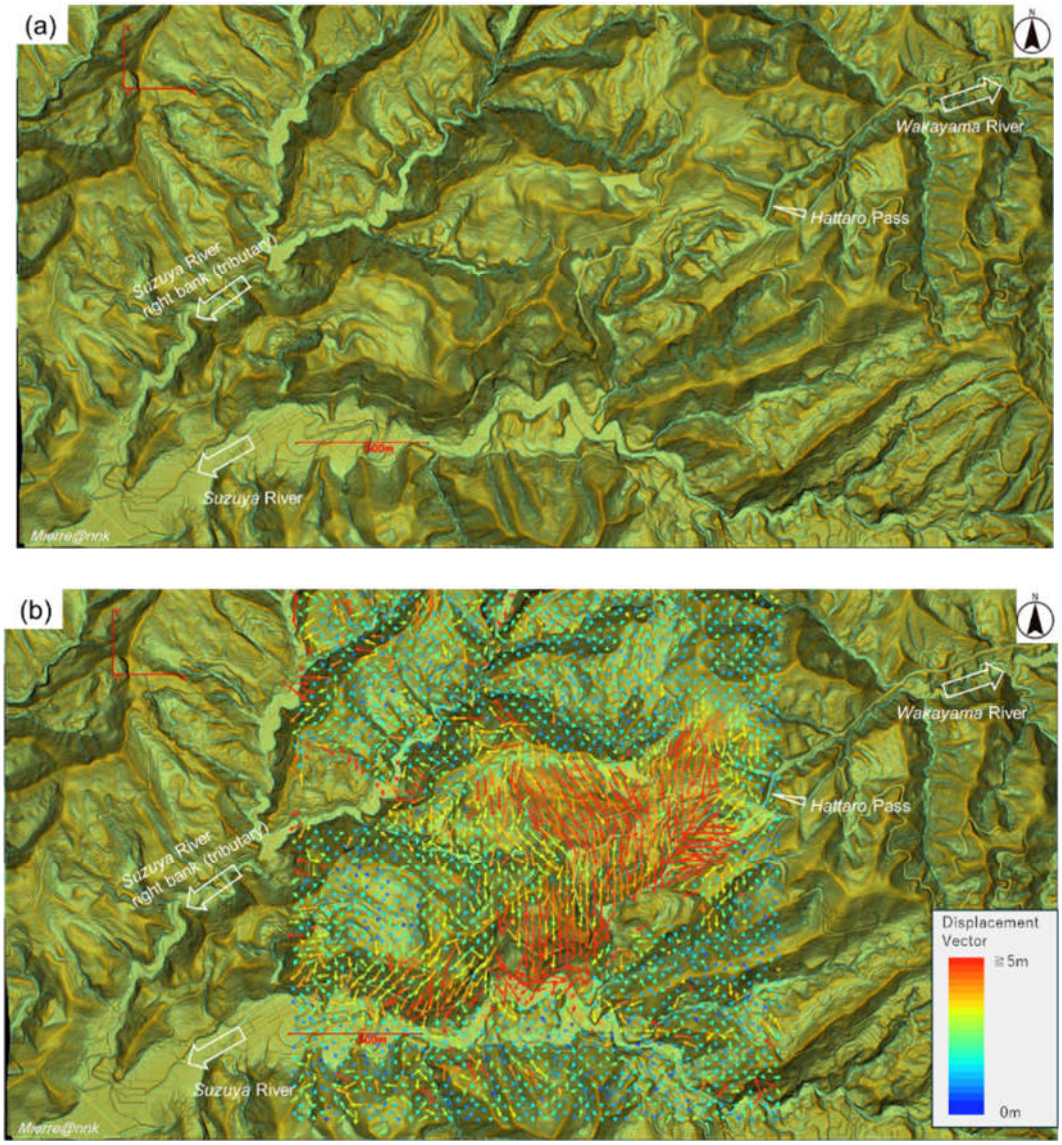

Figure 3. (a) Terrain relief image post- earthquake and (b) Result of displacement vector analysis

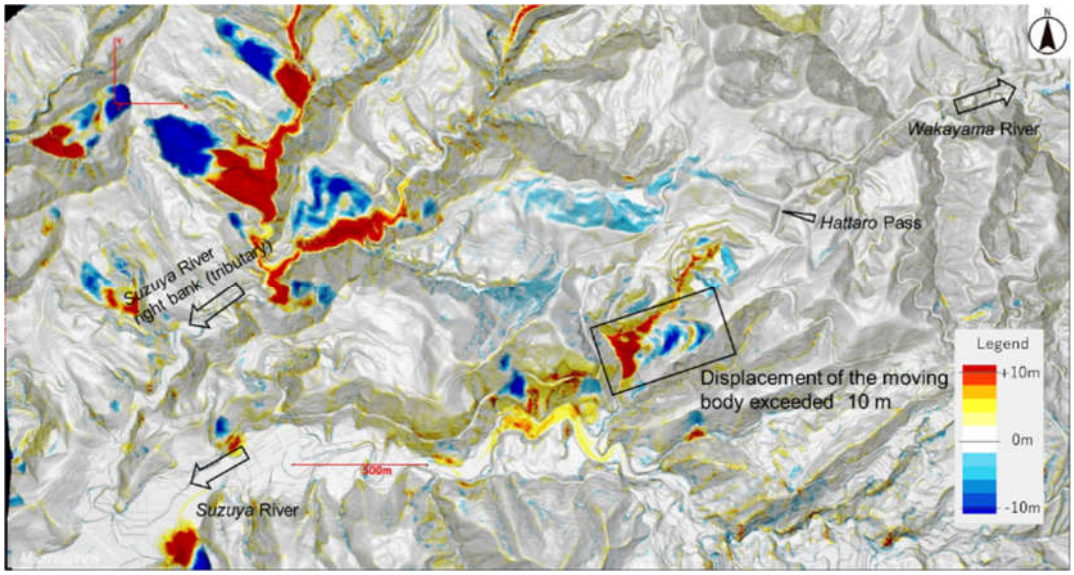

Figure 4. Height difference analysis results and locations where variation of 10 m or more occurred

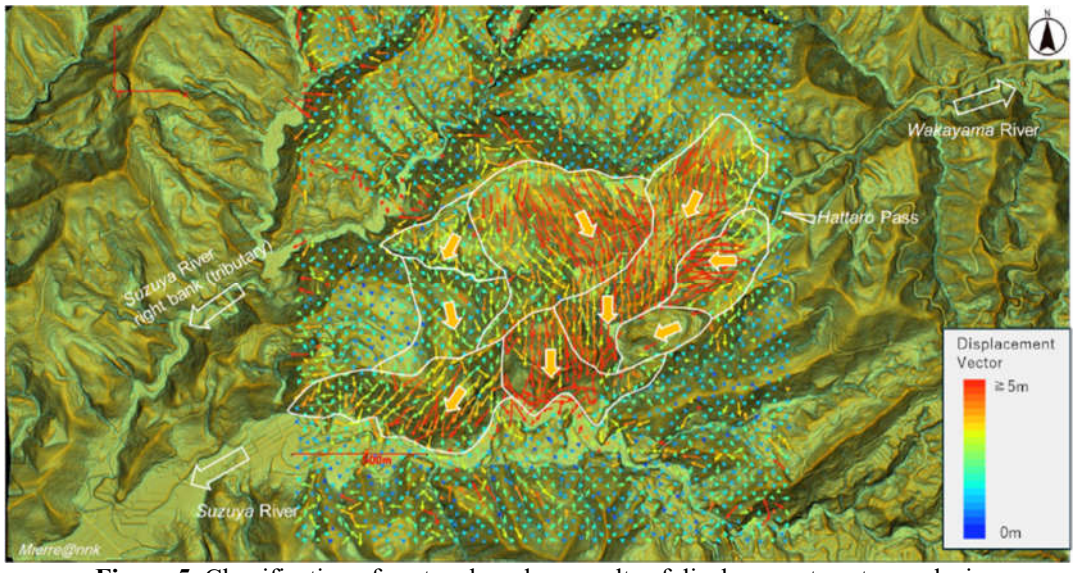

Figure 5. Classification of vectors based on results of displacement vector analysis

5 Field Survey

The field survey was conducted from May 25 to 28, 2024, by members of the Disaster Geology Research Group of the Japan Society of Engineering Geology (JSEG). The route from the *Suzuya* River in *Wajima* City to *Wakayama* Dam via *Hattaro* Pass was surveyed to determine the topographical and geological conditions of the surrounding area. The survey was conducted efficiently after obtaining the results of the analysis of the variation vectors in advance and deciphering the topography (Figure 3). The survey results are shown in Figure 6 and summarized below.

- Loc.I The terrain is a south-falling terrace with a scarps (4 m) behind it (Figure 7).
- Loc.II South-falling terrace crossing a rice paddy field site. The terrain is a south-falling terrain that crosses a paddy field site, suggesting repeated activity. The valley was dammed, and a suitable site for rice paddies was created (Figure 8).
- Loc.III The depression is extensive, reaching a maximum width of 30 m with a step topography of 2.5 m on the north side and 1 m on the south side (Figure 9).

- Loc.IV Multiple terraces are distributed on the steps in the south-falling terrain. Multiple terraces are distributed on the step, and openings were observed at 0.2–1.0 m on each terrace (Figure 10).
- Loc.V Deformed topography (vertical offset of 1.2 m and right lateral offset of 1.6 m) was observed inside the mobile unit (Figure 11).
- Loc.VI The prefectural road overlooking the Suzuya River was completely collapsed (Figure 12).
- Loc.VII A strange slope extrusion phenomenon was observed in the upper part of the prefectural road (Figure 13).

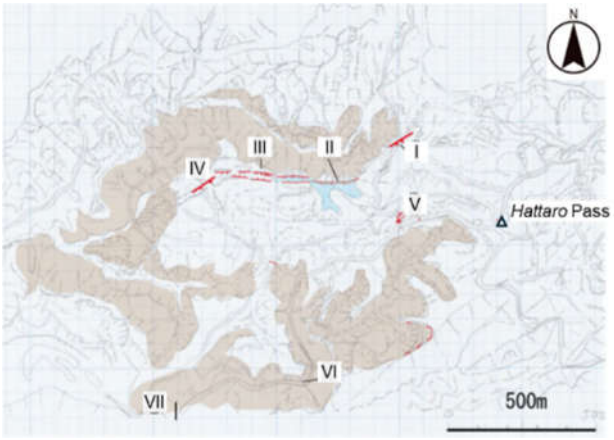

Figure 6. Topographic interpretation map and surveyed locations; red line indicates faults, and red bold line indicates step-like terrain, with the direction of fall indicated by the caption and the direction of movement indicated by the arrow. I-VII: Location number

Figure 7. Image at Loc. I, showing the southward lowering of a step on the west side of *Hattaro* Pass, which occurred approximately 5 m in front of a small cliff topography (4 m high).

Figure 8. Image at Loc. II. Vertical displacement of former rice paddy approximately 2 m W-E, south lowering "fault," the boundary with the rise behind is a small cliff topography. It is believed that repeated activities dammed the valley and created a suitable area for rice paddy fields.

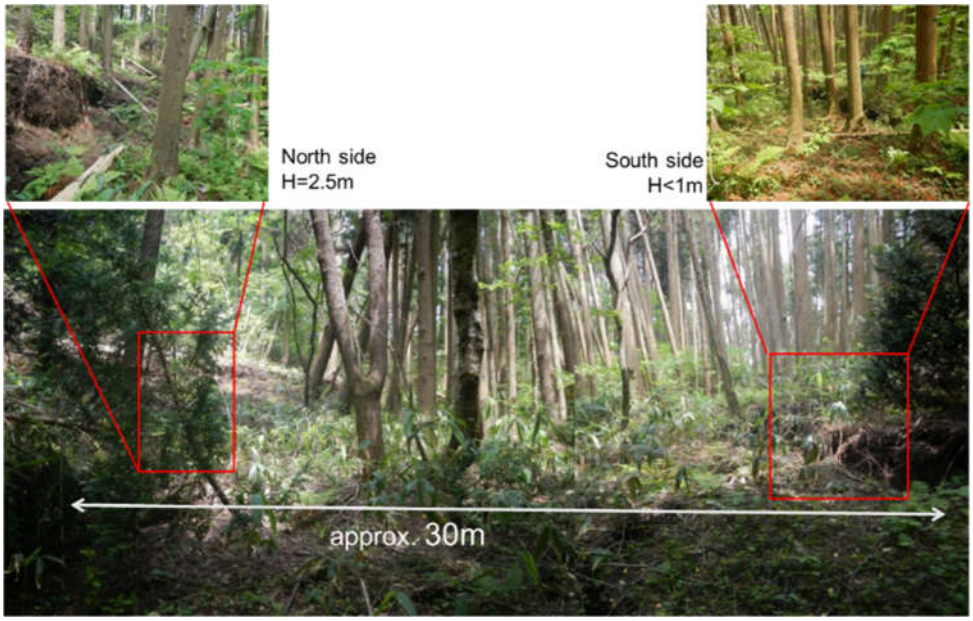

Figure 9. Image at Loc. III. Graben structure is observed.
The north side of the depression is tilted south, and the south side is tilted north.

Figure 10. Image at Loc. IV. Step-fault like deformation of north side of depression and scarps extending to WNW direction

Figure 11. Image at Loc. V. Internal deformation of mobile unit, with 1.2 m longitudinal displacement and 1.6 m horizontal displacement on the right side.

Figure 12. Image at Loc.VI. Collapse of a prefectural road.

Figure 13. Image and Simplified sketch (cross-section) at Loc. VII.
Extruded area at the southern end of the landslide

6 Discussion

Based on the results of the variation vector analysis and survey, the plan, geological structure, and results of the variation vector analysis can be summarized, as shown in Figure 14. The movement trend was significant to the south, orthogonal to the Wakayama-gawa syncline.
Based on a field survey, a series of slip cliffs and graben structures appeared at the northern end of the landslide. These structures have good continuity in the east-west direction, and both are at the edge of the moving landslide body because of the low deformation on the south side. The maximum width of the graben structure was 30 m, and a maximum drop of 2.5 m was observed on the north side. This drop is larger than the 1 m drop on the south side of the graben structure and is the basis for the main slide cliff. Various deformations are observed in the internal structure of the landslide. On the southern side facing Suzuya-River no terraced topography corresponding to a slip cliff was observed. Instead, as shown in Figure 13, extrusion and collapse were observed on many slopes.

The results of vector analysis and field survey were compiled into a cross-sectional map. As shown in Figure 15, the landslide occurred along the stratigraphic plane (10–15°), indicating that the landslide extended from the 30-m wide section of the depression (Loc. III) via the Wakayama-gawa syncline to

the steep slope on the right bank of the Suzuya River (Loc. VII). The movement trend also supports this phenomenon. The field survey revealed multiple traces of sliding. This suggests that the site may be subject to repeated fluctuations owing to the influence of the Wakayama-gawa syncline.

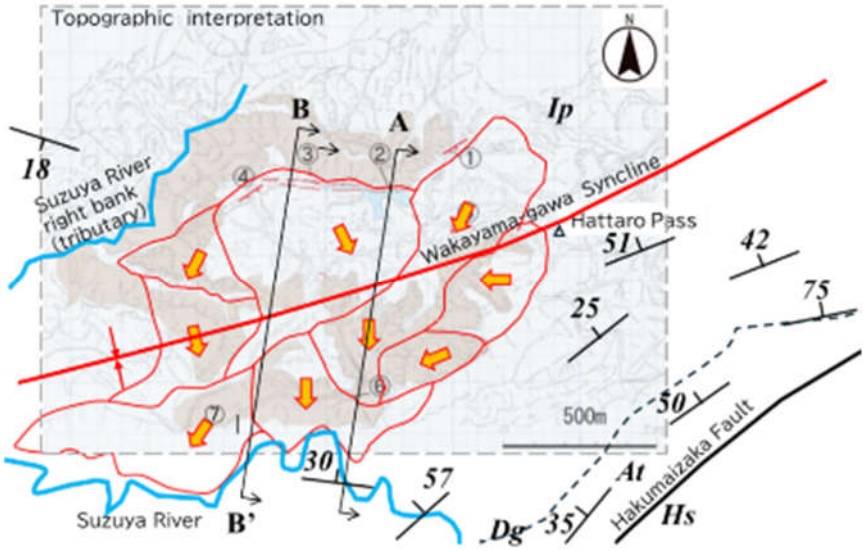

Figure 14. Integrated plan, A-A' and B-B' are cross-sectional locations, legends are same as Figure 3, and red thin line is based on the variation area (Figure 6).

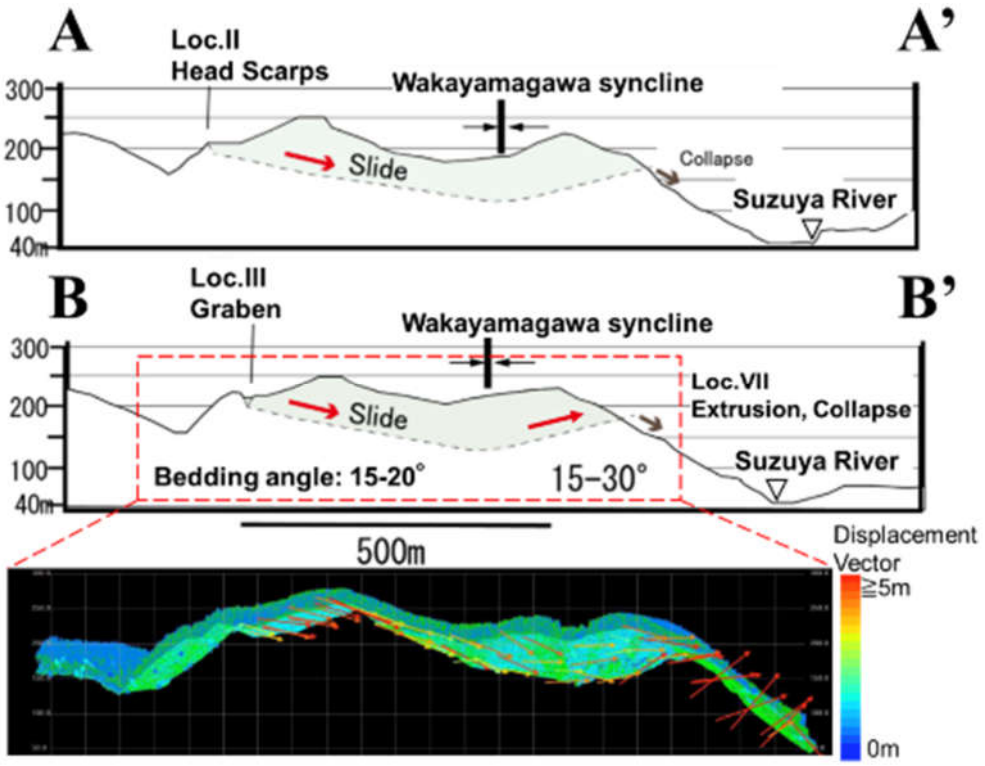

Figure 15. Cross sections of A-A' and B-B' and surrounding area (projected width 100 m)

7 Conclusion

This study confirmed that landslide locations identified through displacement vector analysis from aerial laser surveys matched actual geological phenomena observed after the 2024 Noto Peninsula Earthquake. The displacement vector analysis revealed significant, complex ground deformations. Field surveys

validated these findings. The integration of high-precision aerial data and on-ground surveys is essential for understanding and predicting landslide behaviors, enhancing disaster preparedness and infrastructure stability.

Acknowledgements
This study was supported by the Japan Society for Engineering Geology. Nakanihon Air Co., Ltd. made digital datasets available. Support from both institutions is gratefully acknowledged.

References

Association for Promotion of Infrastructure Geospatial information Distribution: Front Geospatial, https://front.geospatial.jp/ (accessed on 4 July 2024).

Damm, B.; Becht, M..; Varga, K.; Heckmann, T. Relevance of tectonic and structural parameters in Triassic bedrock formations to landslide susceptibility in Quaternary hillslope sediments. *Quaternary International*. 2010, 222(1–2), 143–153.

Fey, C.; Rutzinger, M.; Wichmann, V.; Prager, C.; Bremer, M.; Zangerl, C. Deriving 3D displacement vectors from multi-temporal airborne laser scanning data for landslide activity analyses. *GIScience & Remote Sensing*. 2015, 52(4), 437–461.

Geospatial Information Authority of Japan: Slope Failure and Deposition Distribution Data and Slope Failure and Deposition Distribution Map, https://www.gsi.go.jp/BOUSAI/20240101_noto_earthquake.html (accessed on 4 July 2024).

Karakas, G.; Nefeslioglu, H. A.; Kocaman, S.; Buyukdemircioglu, M.; Yurur, T.; Gokceoglu, C. Derivation of earthquake-induced landslide distribution using aerial photogrammetry: the January 24, 2020, Elazig (Turkey) earthquake. *Landslides*. 2021, 18(6), 2193–2209.

Kikuchi, T.; Hatano, T.; Senda, Y.; Nishiyama, S. Development of analytic method for landslide measurement by movement vectors using S-DEM data obtained from airborne laser point clouds. *Journal of The Japanese Society of Engineering Geology*. 2017, 57(6), 277–288.

Kinoshita, A.; Shibasaki, T.; Hashimoto, J.; HASEGAWA, Y.; SAMMORI, T.; OKADA, Y. Geotechnical characteristics of collapsed slope triggered by the 2008 Iwate-Miyagi Nairiku earthquake in the Koei district, Kurihara City, Miyagi Prefecture, Japan. *Journal of the Japan Society of Erosion Control Engineering*. 2012, 65(2), 3.

Massironi, M.; Zampieri, D.; Superchi, L.; Bistacchi, A.; Ravagnan, R.; Bergamo, A. ; Ghirotti, M. ; Genevois, R. Geological structures of the Vajont landslide. *Italian Journal of Engineering Geology and Environment*. 2013, 573–582.

Mukoyama, S. Estimation of ground deformation caused by the Earthquake（M7.2）in Japan,2008,from the Geomorphic Image Analysis of high resolution LiDAR DEMs. *Journal of Mountain Science*. 2010, 8(2), 239–245.

Osanai, N.; Yamada, T.; Hayashi, S. I.; Kastura, S. Y.; Furuichi, T.; Yanai, S.; ... Miyazaki, M. Characteristics of landslides caused by the 2018 Hokkaido Eastern Iburi Earthquake. *Landslides*. 2019, 16, 1517–1528.

Takami, T.; Mukoyama, S.; Homma, S.; et al. Evaluation and analysis of slope movements using multi-temporal LiDAR DEM. *Journal of the Japan Landslide Society*. 2019, 56(6),295.

Wartman, J.; Dunham, L.; Tiwari, B.; Pradel, D. Landslides in eastern Honshu induced by the 2011 Tohoku earthquake. *Bulletin of the Seismological Society of America*. 2013, 103(2B), 1503–1521.

Yin, Y.; Wang, F.; Sun, P. Landslide hazards triggered by the 2008 Wenchuan earthquake, Sichuan, China. *Landslides*. 2009, 6, 139–152.

Yoshikawa, T.; Kano, K.; Yanagisawa, Y.; Komazawa, M.; Joshima, M.; Kikawa, E. Geology of the Suzumisaki, Noto-iida and Horyuzan district. *in: Quadrangle Series, 1:50,000, Geological Survey of Japan, AIST*. 2002, 76 (in Japanese with English abstract).